Am J Physiol Regul Integr Comp Physiol 294: R1675–R1683, 2008.
First published February, 13, 2008; doi:10.1152/ajpregu.00829.2007.

Circadian rhythm disorganization produces profound cardiovascular and renal disease in hamsters

Tami A. Martino,[1,2,3] Gavin Y. Oudit,[1,2] Andrew M. Herzenberg,[1] Nazneen Tata,[1] Margaret M. Koletar,[3,4] Golam M. Kabir,[2] Denise D. Belsham,[1,3] Peter H. Backx,[2,3] Martin R. Ralph,[3,4] and Michael J. Sole[1,2,3]

[1]*University Health Network, Toronto, Ontario;* [2]*Heart and Stroke/Richard Lewar Centre for Cardiovascular Excellence,* [3]*Departments of Physiology, Medicine, and Psychology, and* [4]*Centre for Biological Timing and Cognition, University of Toronto, Ontario, Canada*

Submitted 16 November 2007; accepted in final form 12 February 2008

Martino TA, Oudit GY, Herzenberg AM, Tata N, Koletar MM, Kabir GM, Belsham DD, Backx PH, Ralph MR, Sole MJ. Circadian rhythm disorganization produces profound cardiovascular and renal disease in hamsters. *Am J Physiol Regul Integr Comp Physiol* 294: R1675–R1683, 2008. First published February, 13, 2008; doi:10.1152/ajpregu.00829.2007.—Sleep deprivation, shift work, and jet lag all disrupt normal biological rhythms and have major impacts on health; however, circadian disorganization has never been shown as a causal risk factor in organ disease. We now demonstrate devastating effects of rhythm disorganization on cardiovascular and renal integrity and that interventions based on circadian principles prevent disease pathology caused by a short-period mutation (*tau*) of the circadian system in hamsters. The point mutation in the circadian regulatory gene, casein kinase-1ε, produces early onset circadian entrainment with fragmented patterns of behavior in +/*tau* heterozygotes. Animals die at a younger age with cardiomyopathy, extensive fibrosis, and severely impaired contractility; they also have severe renal disease with proteinuria, tubular dilation, and cellular apoptosis. On light cycles appropriate for their genotype (22 h), cyclic behavioral patterns are normalized, cardiorenal phenotype is reversed, and hearts and kidneys show normal structure and function. Moreover, hypertrophy does not develop in animals whose suprachiasmatic nucleus was ablated as young adults. Circadian organization therefore is critical for normal health and longevity, whereas chronic global asynchrony is implicated in the etiology of cardiac and renal disease.

circadian; diurnal; tau hamsters; heart disease; renal disease; suprachiasmatic nucleus

IT HAS BEEN RECOGNIZED for decades that circadian rhythms play a dramatic role in the regulation of cardiovascular physiology (7, 16). Moreover, adverse cardiac events (e.g., heart attacks, stroke) show significant day/night (diurnal) variations in both incidence and severity (16), and rhythm disruption is found commonly in patients with sleep apnea, in shift workers, and in transmeridian flight crews, all of whom show higher than average prevalence of cardiovascular disease (2, 6). In animal models, disruption of diurnal rhythms increases mortality in cardiomyopathic hamsters (19) and exacerbates pressure overload myocardial hypertrophy in aortic-banded mice (15).

Circadian rhythm disruption also has been linked with reduced longevity in golden hamsters carrying the circadian period mutation, *tau* (11). The mutant allele reduces the circadian period from ~24 h in the wild type to ~22 h in *tau*/+ heterozygotes (20). Importantly, it is the heterozygotes whose longevity is compromised. When these animals are entrained by 24-h light-dark (LD) cycles, they exhibit phase-advanced onsets of nocturnal behavior with significant fragmentation of diurnal activity (18). Conversely, longevity is increased in aged animals whose disturbed rhythms are reconsolidated by successful grafting of hypothalamic tissue containing the suprachiasmatic nucleus (SCN) (11). Nonetheless, other than the changes in rhythm integrity, the mechanisms underlying the effects on life expectancy have not been explored. Therefore, despite the acknowledged importance of rhythms in health and disease, there are virtually no experimental data prospectively demonstrating a causal link between circadian dysregulation and organ pathology. In this study, we hypothesize that altered circadian organization plays a role in genesis of severe cardiac and renal disease, leading to early death in +/*tau* mutant hamsters.

MATERIALS AND METHODS

Animal housing and locomotor behavior recording. All animals are housed at the University of Toronto zoology animal facility. This investigation conforms to the *Guide for Care and Use of Laboratory Animals* published by the United States National Institutes of Health (NIH Publication No. 85–23, revised 1996), and is approved by the Canadian Council on Animal Care. The hamsters (*Mesocritetus auratus*; *tau*) have been maintained in the breeding colony in a LD 14:10 cycle since 1991, and the colony is outbred every second generation with a wild type obtained from Charles River Laboratories. Activity is recorded from individual cages equipped with running wheels as required using the Dataquest II data acquisition system coupled with ActiView Biological Rhythm Analysis version 1.2 (Minimitter, Bend, OR). Genotype is confirmed by PCR analysis of the *casein kinase 1 epsilon* gene.

SCN ablation. Electrolytic lesions of the SCN are produced using electrodes aimed at the SCN placed stereotaxically on midline under deep pentobarbital anesthesia. Coordinates are as follows: anterior position +0.6 mm from bregma and −0.8 mm from dura. Lesions are small, and nearby structures (medial preoptic nucleus; subparaventricular zone, optic chiasm) are spared. Placement is verified by the lack of 24-h rhythmicity in subsequent behavioral records and by histological examination.

Echocardiography. Echocardiography is performed in a blinded manner on all hamsters at 4 and at 17 mo of age. All animals are housed on a 24-h LD cycle (14:10) throughout, or for those on alternative cycles they are returned to LD 14:10 3 wk before final cardiovascular assessments. Animals are anesthetized with 2% isoflurane gas delivered through a nose cone and are maintained at a body temperature of 37°C using a heating pad. Transthoracic echocardiog-

Address for reprint requests and other correspondence: M. J. Sole, 4N-488 Toronto General Hospital, 585 Univ. Ave., Toronto, Ont., Canada M5G 2N2 (e-mail: michael.sole@uhn.on.ca).

The costs of publication of this article were defrayed in part by the payment of page charges. The article must therefore be hereby marked "*advertisement*" in accordance with 18 U.S.C. Section 1734 solely to indicate this fact.

raphy is performed with Sequoia (Acuson, Mountain View, CA) using a 13-MHz linear array probe. Two-dimensional M-mode images are acquired while the animal is in a semiconscious state (0.75% isoflurane) using High Resolution Zoom with a sweep speed of 200 mm/s, from the short axis view at the papillary muscle level. Measurements include left ventricular (LV) end-diastolic (LVEDD) and end-systolic (LVESD) diameter, LV diastolic anterior and posterior wall thickness, percent fractional shortening (%FS), and heart rate.

Hemodynamic studies. In vivo hemodynamic measurements are performed in a blinded manner on animals anesthetized with 1.5% isoflurane gas. Body temperature and heart rate are continuously monitored and maintained. The right common carotid artery is exposed and cannulated using a 1.4-Fr. microtip catheter (Millar), which is then fed to the proximal aorta and left ventricle for respective measurements. Data are acquired using the MP100 hardware imaging system and analyzed using Acqknowledge version 3.7.3 (Biopac Systems). Data are analyzed for aortic systolic and diastolic blood pressure, mean arterial blood pressure, LV pressure measurements [LV end-systolic and end-diastolic (LVEDP) pressure], and the maximum (LVdP/d$t_{\max}$) and minimum first derivatives of LV pressure.

Histology and pathological assessment of hamsters. Animals are anesthetized and killed, and tissues were collected. For histological assessment, tissues are fixed in 10% formalin and paraffin-embedded. Heart sections taken at the level of the papillary muscle are stained with hematoxylin and eosin (H&E; Sigma), Massons trichrome, or Picrosirius red (PSR; Fluka). Kidney sections are stained with H&E, PSR, or Period acid-Schiff. We determined in a blinded manner the general tissue morphology, myocyte cross-sectional area, and extent of interstitial fibrosis. Sections are digitally imaged using the Nikon microphot-FXA microscope, along with the Nikon ACT-1 version 2.62, or ImageJ 1.33u (National Institute of Health) software.

Electron microscopy glomerular analyses. Glomerulosclerosis, tubular hyperplasia, and renal fibrosis are assessed using pathological cross sections. For electron microscopy of renal glomeruli, kidneys are fixed in buffered 1% glutaraldehyde-4% formaldehyde, postfixed in 1% osmium tetroxide, and embedded in Epon-araldite. Ultrathin sections stained with uranyl acetate and lead citrate are examined using a transmission electron microscope (1200EX-II; Jeol Peabody).

In situ end labeling assay (terminal uridine deoxynucleotidyl transferase dUTP nick end labeling). DNA-damaged cells are detected by terminal uridine deoxynucleotidyl transferase dUTP nick end labeling (TUNEL) assay, adapted to an automated in situ hybridization instrument (Discovery Ventana Medical Systems, Tucson, AZ). We use 5-μm-thick deparaffinized tissue sections, digestion with Protease I (Ventana Medical), recombinant terminal deoxynucleotidyl transferase (GIBCO-BRL), and Biotin 16-dUTP (Roche Diagnostics), in

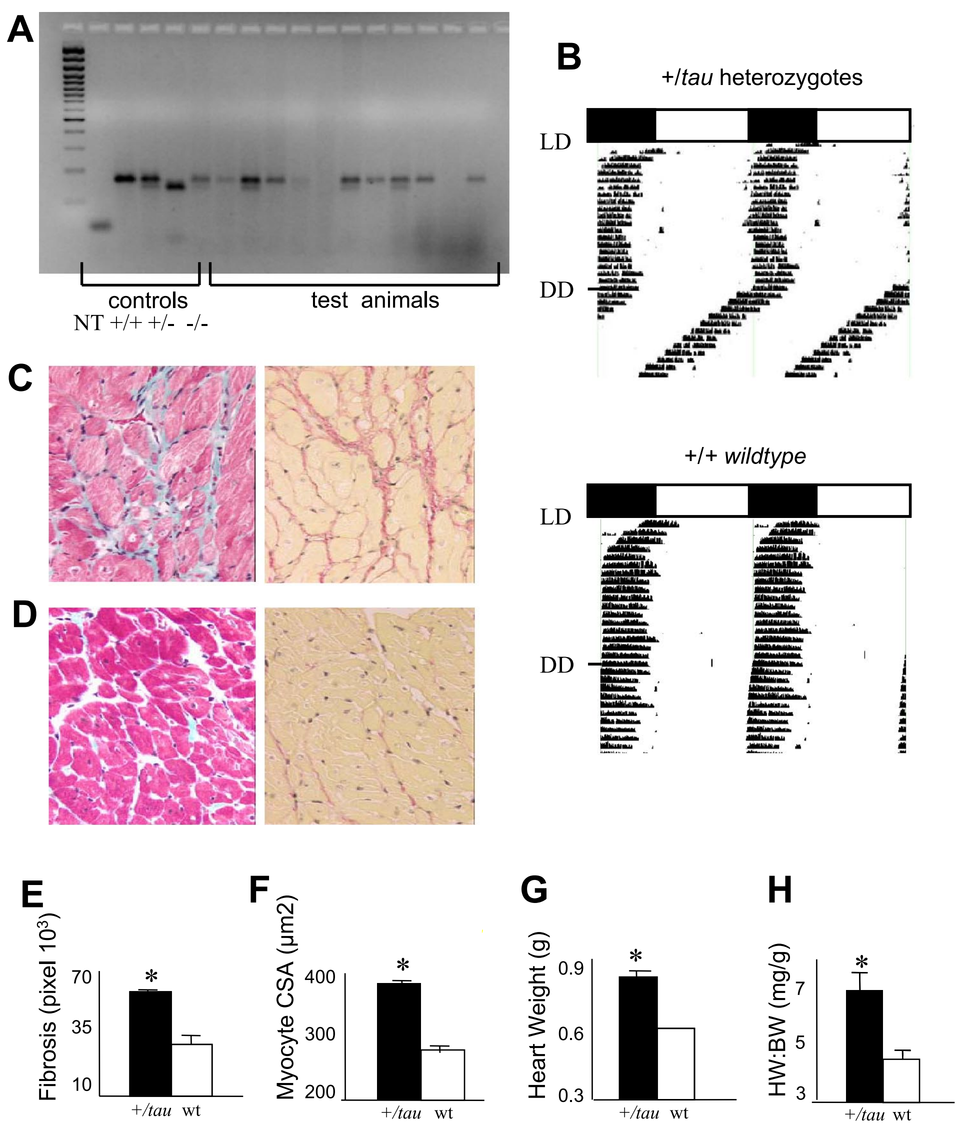

Fig. 1. Development of profound cardiac hypertrophy in hamsters carrying the circadian period mutation (*tau*/+). *A*: representative genotype vs. circadian phenotype shows wild type (wt), *tau*/+, and *tau*/*tau* hamsters analyzed for the mutation in the casein kinase-1-ϵ (*ck1*ϵ), on 1% ethidium bromide (EtBr) agarose gel analysis. *B*: representative phenotype by activity analysis shows earlier-onset and fractured activity pattern in *tau*/+ hamsters (*left*) entrained to a 14:10-h light-dark (LD) cycle and a reduced 22- circadian period in total darkness (DD; <4 lux) compared with wt (24 h, *right*). *C*: representative images of hearts from *tau*/+ show extensive pathology, widespread myocyte hypertrophy *(C, left* Masson's trichrome), and myocardial fibrosis *(C, right* Picrosirius red). *D*: representative images from wt hearts *(D, left* and *D, right)* shown at the same magnification, which have no obvious signs of pathology. *E*: digital quantification demonstrates significant myocardial fibrosis (n = 10, $P < 0.01$) in *tau*/+ heart. *F*: increased myocyte cross-sectional area (MCSA) (n = 40, $P < 0.05$) in *tau*/+ hearts. *G*: increased heart weight in *tau*/+ animals. *H*: heart-to-body weight ratio consistent with development of gross cardiac hypertrophy. Values are listed in Tables 1–3.

Table 1. *Echocardiographic, hemodynamic, and morphometric parameters in tau/+ mutant hamsters (17 mo of age)*

	tau/tau	*tau/+* (14:10)	*tau/+* (12:10)
n	8	8	8
HR, beats/min	413±8	422±11	404±13
AW, mm	1.18±0.02	1.15±0.03	1.16±0.04
LVEDD, mm	5.82±0.06	6.36±0.11*	5.48±0.12‡
LVESD, mm	3.13±0.09	4.47±0.05*	3.07±0.08‡
FS, %	46.3±1.3	29.7±2.4*	43.9±2.4‡
VCFc, circ/s	8.36±0.26	4.95±0.54*	8.05±0.31‡
PAV, cm/s	89±2	73.9±1.8*	88±3.1‡
SBP, mmHg	146±3	117±5*	150±3‡
DBP, mmHg	94±3	68±4*	93±1‡
MABP, mmHg	111±3	84±4*	112±2‡
$+dP/dt_{max}$, mmHg/s	9,987±441	6,118±373*	9,182±331‡
$-dP/dt_{max}$, mmHg/s	9,929±396	6,003±271*	9,226±946‡
LVEDP, mmHg	3.8±0.8	10.4±1.5*	−5.2±0.7‡
BW, g	138±2.4	124±7.6	131±1.7
HW/BW, mg/g	4.37±0.09	6.58±0.52*	5.15±0.16‡
HW/TL, mg/mm	26.4±1.1	35.7±1.5*	32.2±0.6‡
KW/BW, mg/g	5.02±0.21	5.81±0.41	5.06±0.13
KW/TL, mg/mm	29.2±1.8	31.2±1.6	31.7±0.4
Cardiac fibrosis, pixels	28,783±9,614	58,132±7,928†	36,879±3,740‡
MCSA, μm^2 (n = 40)	271±6.2	366±9.6*	310±8.7‡

Values are means ± SE; *n*, no. of hamsters. Comparative data for *tau/tau* are illustrated in Fig. 4, *E-H*. HR, heart rate; AW, anterior wass; LVEDD, left ventricular end-diastolic dimension; LVESD, left ventricular end-systolic dimension; FS, fractional shortening (LVEDD − LVESD)/LVEDD × 100); VCFc, velocity of circumferential shortening (FS/aortic ejection time); PAV, peak aortic velocity; SBP, systolic blood pressure; DBP, diastolic blood pressure; MABP, mean arterial blood pressure; dP/dt_{max}, maximum first derivative of left ventricular pressure; LVEDP, left ventricular end-diastolic pressure; BW, body wt; HW/BW and KW/BW, heart wt-to-body wt and kidney wt-to-body wt ratios, respectively; HW/TL and KW/TL, heart wt-to-tibial length and kidney wt-to-tibial length ratios, respectively; MCSA, myocyte cross-sectional area. *P < 0.01 and †P < 0.05 compared with all other groups (wild type, *tau/+*, and *tau/tau*). ‡P < 0.05, 17 mo *tau/+* (12:10-h light-dark cycle) compared with 17 mo *tau/+* (14:10-h light-dark cycle).

accordance with well-established protocols. Colormetric visualization uses avidin-horseradish peroxidase and 3,3′-diaminobenzidine, with hematoxylin counterstain.

Immunohistochemistry. Immunohistochemistry for CD3 (Dako, Carpinteria, CA) is performed on the NEXES autoimmunostainer (Ventana Medical Systems) at a dilution of 1:200, in accordance with the manufacturer's specifications. Immunodetection is carried out using a 1:100 dilution of biotinylated anti-rabbit IgG (Vector Laboratories, Burlingame, CA) and the Ventana 3–3′-diaminobenzidine detection system. Tissue sections are heated before immunostaining, blocked with endogenous biotin (Ventana Avidin/Biotin Block), and finally counterstained with hematoxylin.

Proteomics and mass spectrometry: protein analyses, SDS-PAGE, trypsin digestion, and electron spray ionization in an LCQ DECA XP ion trap mass spectrometer. Protein content of each sample is determined using the Bradford Assay method (Bio-Rad Laboratories). Urinary protein content is analyzed on 10–20% tricine gels (Invitrogen) stained with Coomassie dye for 20 min. Selected bands are prepared for mass spectrometry/mass spectrometry (MS/MS) by excision from the gel and digested overnight in 50 μl buffer containing 50 mM HN_4HCO_3, 10% acetonitrile, and 10 ng/μl sequencing-grade trypsin (Roche). The MS/MS analysis of tryptic peptides is performed using a LCQ DECA XP ion trap (Thermo Finnigan). *Buffer A* for liquid chromatography contains 0.1% formic acid, and *buffer B* contains 99.9% acetonitrile and 0.1% acetic acid. Samples are injected at a rate of 10 μl/min on a Vydac reverse-phase column (0.2 × 150 mM; Grace Vydac, Hesperia, CA) over 5 min in 5% *buffer B* using an Agilent 1100 Series CAP-LC. Peptides are eluted over a 10–65% *buffer B* gradient for 40 min at a rate of 2 μl/min for detection by LCQ DECA XP mass spectrometry. Data analysis is performed by Sequest (Lisle, IL) software with raw files searched against hamster, murine, and human databases on NCBI (www.ncbi.nlm.nih.gov/). Positive identifications are made when two or more peptides with Xcorr > 2.5 (+2 ions) or 3.7 (+3 ions) match to the same protein. Protein identification is validated as required, using Western blot analysis on nitrocellulose membrane and chemiluminescent detection (Amersham Biosciences).

Plasma biochemistry and kidney function analysis. Blood samples are collected from anesthetized hamsters at zeitgeber 1–16, and 200 μl of plasma are used for measurement of plasma Na^+, K^+, Cl^-, ionized Ca (Ca^{2+}), lactate, glucose, urea, and creatinine using a Stat Profile M7 Analyzer (Nova Biomedical, Waltham, MA).

Statistical analyses. Data are expressed as means ± SE. Statistical comparisons are made either by use of the independent Student's t-test for comparing individual groups or by one-way ANOVA followed by Tukey's multiple test for comparisons of more than two groups. Analysis is performed using SPSS statistical software (version 12.0.0). Results of $P < 0.05$ are considered statistically significant.

RESULTS

We postulated that chronic circadian disorganization like that seen in *tau/+* animals on 24-h LD cycles results in pervasive physiological impairments leading to an early demise. To test this, we focus specifically on the cardiovascular system where robust diurnal or circadian cycling of gene expression already has been shown (14, 21, 23, 24) and wherein a pathological effect of rhythm disturbance has been implicated in human beings (7, 16). All animals are genotyped using an ear tip for DNA analyses (genotyping; Fig. 1*A*) and phenotyped using conventional behavioral analyses [*tau/+* (Fig. 1*B*, *left*) and wild types (Fig. 1*B*, *right*)].

We first perform autopsy examination of animals at 17 mo of age, close to the limit of the shortened life span of the *tau/+* hamsters (11). This reveals a marked cardiomyopathy consistent with our hypothesis. Histopathology reveals extensive

Table 2. *Echocardiographic, hemodynamic, and morphometric parameters in young tau hamsters*

	tau/tau	*tau/+*
	6	6
HR, beats/min	404±6	411±5
AW, mm	0.98±0.05	1.03±0.06
LVEDD, mm	5.19±0.1	5.41±0.11
LVESD, mm	2.84±0.11	3.08±0.09
FS, %	45.8±1.8	43.1±3.1
VCFc, circ/s	8.52±0.36	8.22±0.63
PAV, cm/s	85±3.5	82±2.8
SBP, mmHg	135±5	147±3
DBP, mmHg	87±4	97±2
MABP, mmHg	103±4	114±2
$+dP/dt_{max}$, mmHg/s	10,942±591	8,595±636
$-dP/dt_{max}$, mmHg/s	10,920±400	7,425±1,807
LVEDP, mmHg	−1.3±0.9	0.5±1.7
BW, g	113±5.2	113±3.7
HW/BW, mg/g	4.91±0.13	4.72±0.2
HW/TL, mg/mm	24.33±1.9	23.25±1.1
KW/BW, mg/g	5.3±0.28	5.38±0.25
KW/TL, mg/mm	26.1±2.1	26.78±1.9
Cardiac fibrosis, pixels	8,698±435	9,013±481
MCSA, μm^2 (n = 40)	239±10.3	256±8.5

Values are means ± SE; *n*, no. of hamsters. All hamsters were 4 mo old.

Table 3. *Plasma biochemistry in tau hamsters*

	Na^+, mM	K^+, mM	Cl^-, mM	Ca^{2+}, mM	Lactate, mM	RBG, mM	Urea, mM	Cr, mM
17 Months old								
tau/+	140.5±1.4	6.12±0.38*	102.5±0.8	1.22±0.04	5.21±0.47	9.45±0.9	6.8±0.56	112.4±8.1*
tau/*tau*	138.8±0.7	5.06±0.11	101.2±0.5	1.21±0.02	6.06±0.41	9.23±0.89	6.36±0.67	72.5±2.7
4 Months old								
tau/+	139.3±0.5	5.0±0.2	104.0±0.49	0.77±0.04	9.8±0.32	13.71±1.1	7.6±0.29	69.6±4.68
tau/*tau*	137.3±1.1	4.8±0.2	105.3±1.6	0.87±0.05	8.7±0.72	10.21±1.06	7.2±0.35	78.9±6.67

Values are means ± SE; $n \geq 7$ hamsters/time point. RBG, random blood glucose. Blood samples were collected from anesthesized hamsters at ZT12-16, and 200 μl of plasma were used for measurement of plasma Na^+, K^+, Cl^-, Ca^{2+}, lactate, glucose, urea, and creatinine using a Stat Profile M7 Analyzer (Nova Biomedical, Waltham, MA). $*P < 0.01$ compared with all other groups.

interstitial fibrosis (Fig. 1*Ci*) and widespread collagen deposition in the extracellular matrix (Fig. 1*Di*) in the myocardium of *tau*/+ animals compared with the wild types. The adverse remodeling is digitally quantified and is significantly increased in *tau*/+ hearts compared with the wild type (Fig. 1*E* and Table 1). We recognize that an ideal method for quantification of myocardial fibrosis is performed by measuring the volume fraction of myocardium occupied by collagen tissue; the pixels approach only estimates the extent of fibrosis that occurs. However, volume fractionation was not feasible in the current setting; moreover, since the interstitial fibrosis is so pervasive in the *tau*/+ hearts and virtually nonexistent in all the other groups, the rough measure should suffice to show relative intensity and scale. We also note widespread myocyte hypertrophy in *tau*/+ hearts, as evidenced by pathological staining (Fig. 1, *Ci* and *Di*) and by quantification (Fig. 1*F* and Table 1).

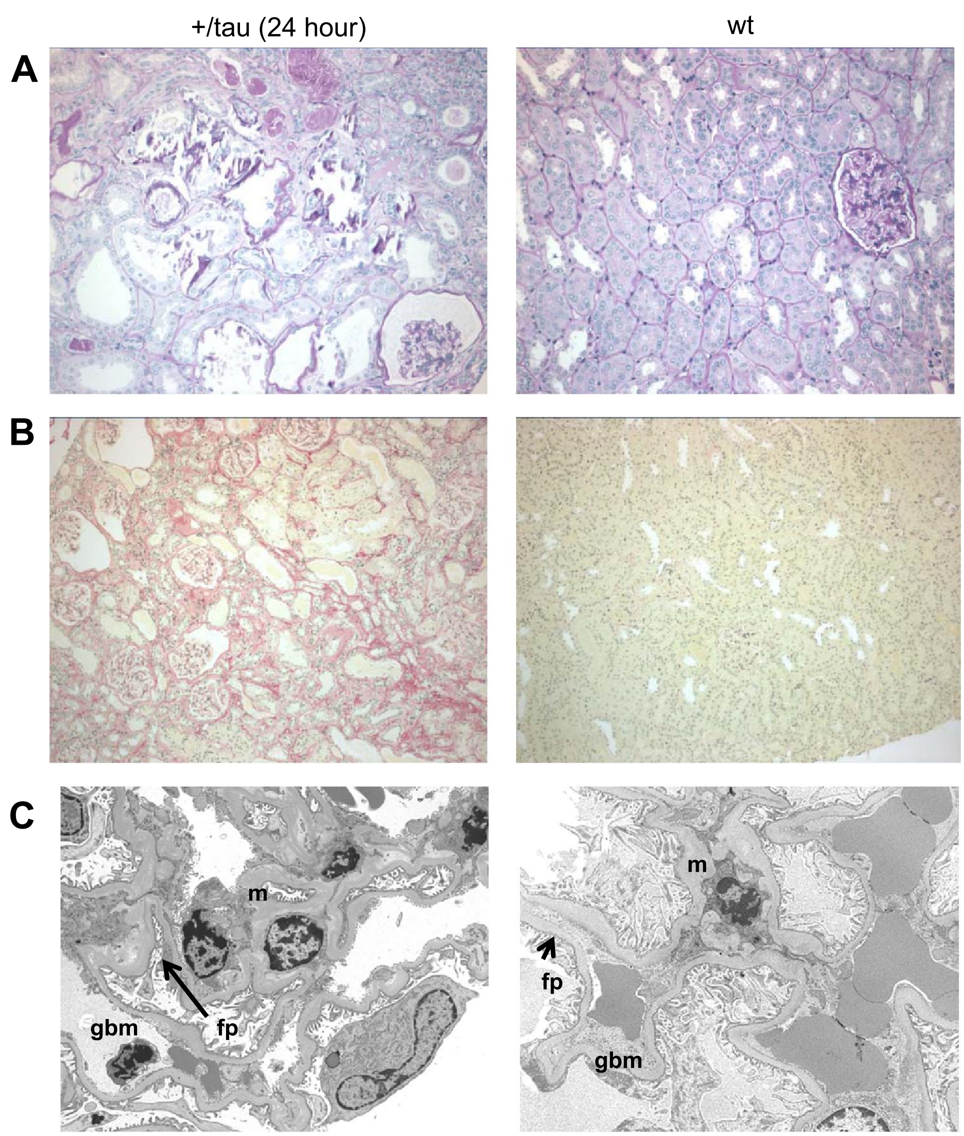

Fig. 2. The *tau*/+ have severe heart disease and evidence of underlying kidney disease. Renal pathology in *tau*/+ (*left*) vs. wt (*right*), showing tubular dilatation in *tau*/+ kidney (Periodic acid stain; *A*), and widespread fibrosis with collagen deposition in *tau*/+ kidney (Picrosirius red) (*B*). *C*: electron microscopy shows glomerular ischemia but no evidence of immune-type deposits in *tau*/+ kidney. This is consistent with development of primary renal disease and helps exclude infection or autoimmune activity as cause.

In addition, the heart weight (Fig. 1*G*) and heart weight-to-body weight ratios (Fig. 1*H*) are significantly increased in *tau*/+ hearts (also see Table 1). Thus, collectively, these findings show the development of obvious hypertrophy and extensive pathological remodeling in the *tau*/+ heart.

To evaluate cardiac function, we perform in vivo catheterization and hemodynamics and document significant deterioration in *tau*/+ heart vs. the wild type (Table 1). This includes: *1*) markedly decreased systolic, diastolic, and mean arterial blood pressure ($P < 0.01$) indicative of hypotension in the *tau*/+ animals; *2*) significantly increased LVEDP consistent with diastolic dysfunction in the heart ($P < 0.01$); and *3*) reduced (40%) dP/dt_{max} and $-dP/dt_{max}$ values, showing significantly impaired myocardial contractility ($P < 0.01$). Impaired cardiac function is confirmed using transthoracic echocardiography (Table 1). LVEDD and LVESD are significantly increased, and ventricular FS, a mathematical measure of systolic function, is greatly reduced from 46.3% (wt) to 29.7% (*tau*/+) ($P < 0.01$). Flow parameters measured as velocity of circumferential shortening and peak aortic velocities are also significantly reduced, consistent with the hypotension ($P < 0.01$). Thus these data show that, in addition to profound pathological findings in the hearts of *tau*/+ animals, the physiology reflects severe myocardial hypertrophy and dysfunction, leading to cardiomyopathy and heart failure.

We then exclude the possibility that the cardiac phenotype in the *tau*/+ animals is the result of a pleiotropic gene effect. Consistent with this notion, cardiopathology was restricted to the heterozygotes. The homozygous *tau*/*tau* hamsters (period = 20 h) retain consolidated patterns of behavior, are unable to synchronize with 24-h days (and thus do not show the same circadian dysregulation as the *tau*/+ hamsters do), and

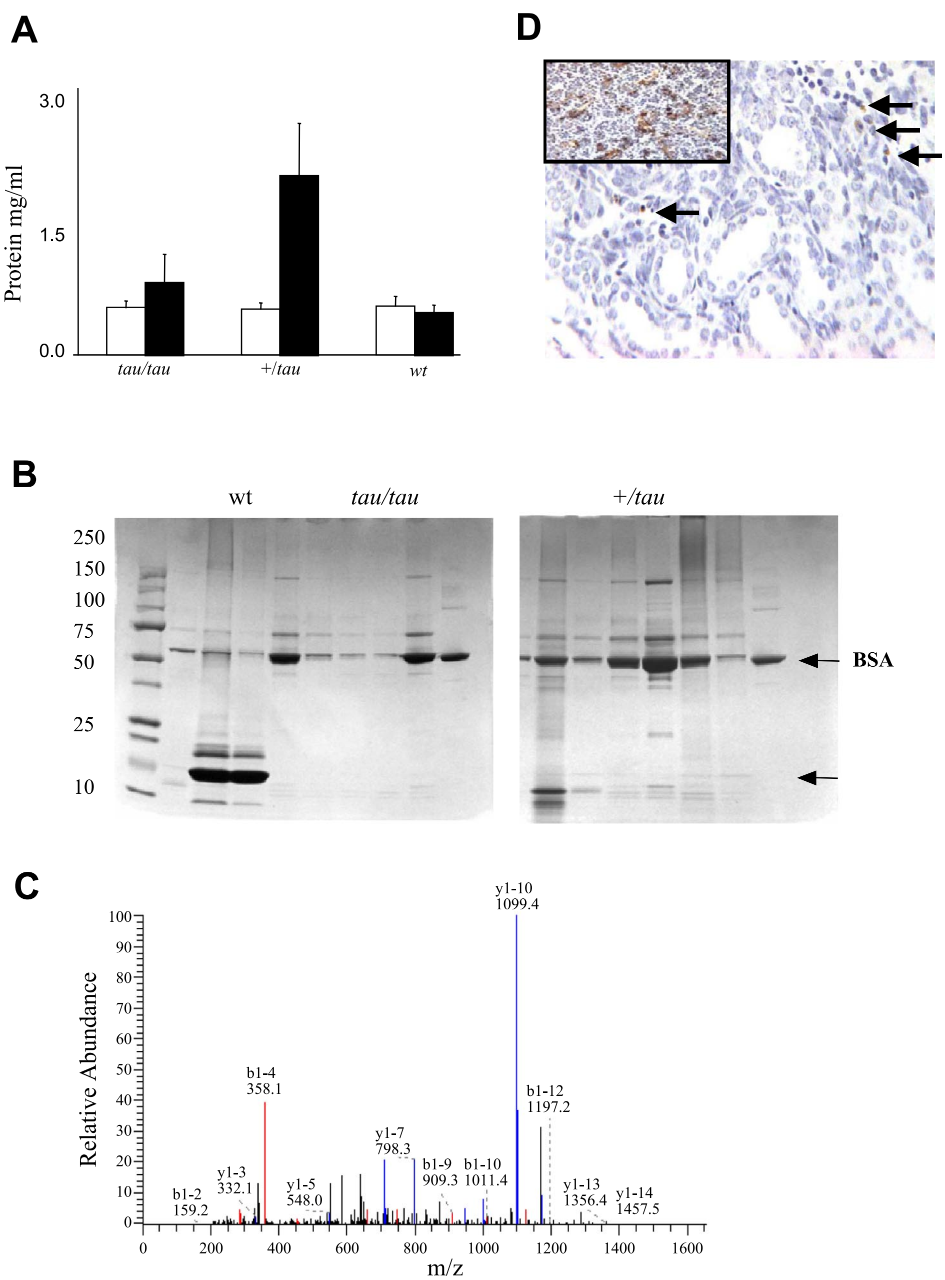

Fig. 3. Mass spectrometry proteomics and apoptosis in *tau*/+ kidneys. *A*: proteinuria in *tau*/+ urine by 17 mo of age (open bars = 4 mo, filled bars = 17 mo of age). *B*: representative urine samples analyzed by gel electrophoresis revealing the presence of both high- and low-molecular-mass proteins in the *tau*/+ urine. First lane is marker, and subsequent lanes represent different animals. Arrow *top right* is albumin, arrow on *bottom right* points to an ~15-kDa protein band appearing characteristically in urine of *tau*/+ animals. This band is excised, trypsin digested, and subject to mass spectrometry (MS) analyses. *C*: representative MS/MS spectrum for the 15-kDa band, identified by MS as *cytochrome c*, a marker of apoptosis. *D*: terminal uridine deoxynucleotidyl transferase dUTP nick end labeling (TUNEL) staining revealing apoptosis in *tau*/+ mutant kidney ($n > 3$). Apoptosis was detected in kidney sections taken from the aging tau heterozygote hamsters. Apoptosis was not detected in age-matched wild-type kidney sections. *Inset*, positive control using murine thymus.

importantly, do not develop pathology nor declining cardiac function like heterozygotes. Furthermore, young *tau*/+ hamsters (4 mo of age and easily assessed by actigraphy) appear healthy, with all cardiovascular parameters including cardiac pathology, hemodynamics, and echocardiography similar to the wild types (Table 2, also see Fig. 4 below). Although this does not definitively disclude congenital conditions, they are certainly not obvious. Moreover, it suggests the cardiomyopathy that develops in *tau*/+ animals does so only over an extended period of circadian dysregulation. In the aggregate then, abnormal circadian entrainment appears to act as a procardiomyopathic stimulus, and the heart decompensates over time.

We also measure plasma biochemistry and detect elevated K^+ and creatinine levels, specifically in the 17-mo-old *tau*/+ mutants (Table 3), but no changes in other plasma values including normal glucose levels. These findings suggest that the *tau*/+ animals with severe heart disease may also have underlying kidney disease. Indeed, we observe severe renal pathology in the *tau*/+ mutants, including proximal tubular dilatation with degenerative and regenerative changes; the glomeruli show ischemic change (Fig. 2*A*) and active fibrosis or collagen deposition throughout the renal cortex (Fig. 2*B*). However, the basement membrane thickness appears normal, and there are no immune-type electron-dense deposits, thus indicating that the renal disease is primary in origin and not likely because of infectious or autoimmune processes (Fig. 2*C*).

The aging *tau*/+ also exhibit proteinuria compared with all other groups. This is analyzed by determining protein concentration in the urine of all the tau hamster phenotypes, and at both early (4 mo) and late (17 mo) ages (Fig. 3*A*). Next, we ran SDS-PAGE, revealing the presence of both high- and low-molecular-mass proteins in urine of the aging (17 mo) *tau*/+

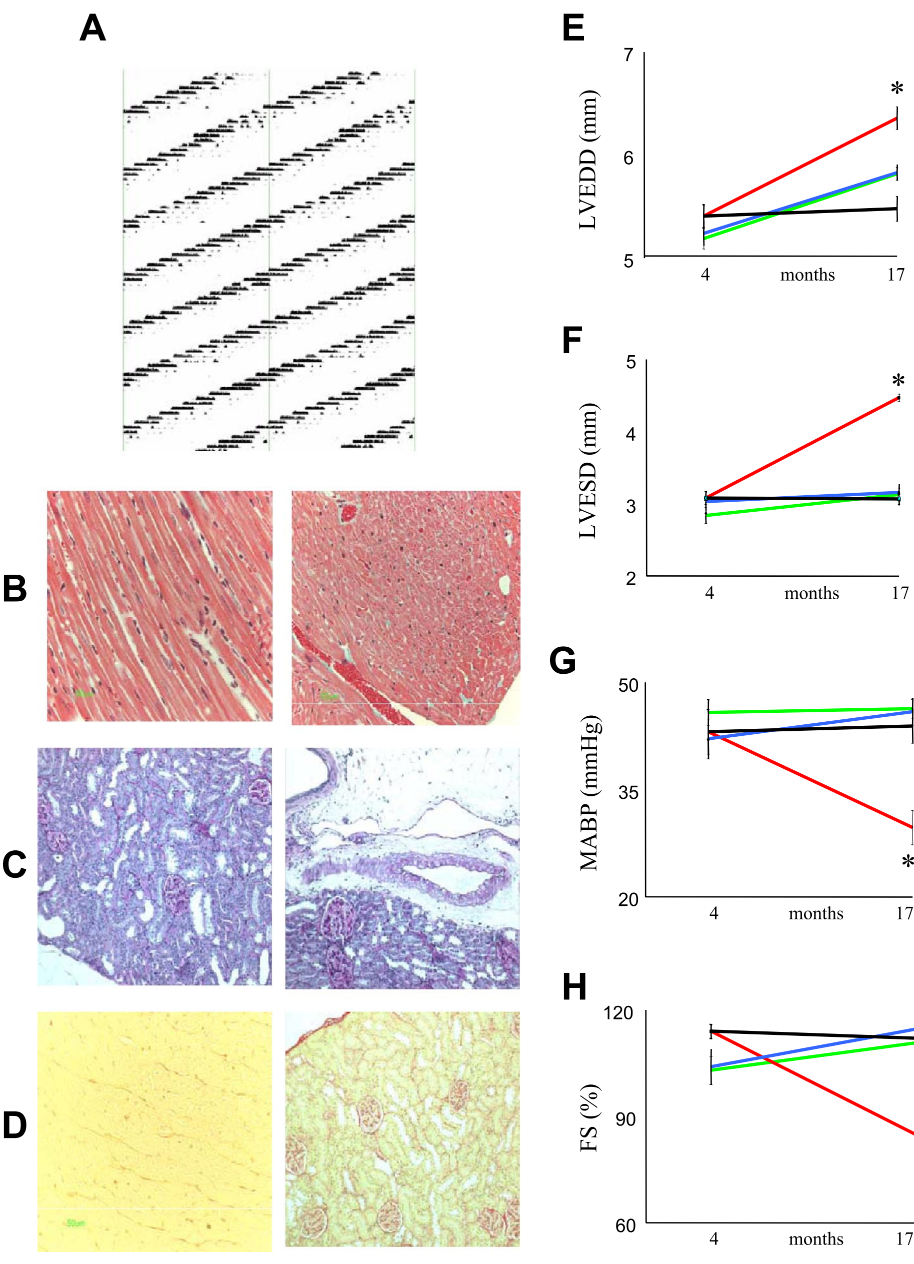

Fig. 4. Rescue of circadian disturbance protects against the cardiac disease phenotype. *A*: representative locomotor activity showing a tau of 22 h for *tau*/+ in 12:10 LD. *B*: normal cardiac histological sections from aged *tau*/+ maintained on a phenotype-appropriate 22-h LD; these animals exhibit healthy myocardium (Masson's trichrome). *C*: renal pathology is also normal, as shown here from aged *tau*/+ maintained on a phenotype-appropriate 22-h LD cycle (Periodic acid stain). *D*: renal histological sections from aged *tau*/+ on 22-h LD, further revealing no evidence of fibrosis or collagen deposition; the kidneys appear normal (Picrosirius red). *E-H*: cardiac indexes in aged *tau*/+ maintained in 22-h LD. *E*: normal left ventricular end-diastolic dimensions (LVEDD, mm) in 22 h *tau*/+ at 17 mo of age. *F*: normal left ventricular end-systolic dimensions (LVESD, mm) in 22 h *tau*/+ at 17 mo of age. *G*: normal mean arterial blood pressure (MABP, mmHg) with no evidence of hypotension in 22 h *tau*/+ at 17 mo of age. *H*: %fractional shortening (%FS) in 22 h *tau*/+ revealing normal contractility, consistent with hemodynamic and morphometric parameters. All phenotypes tested are shown, with black lines = 22 h *tau*/+, red = 24 h *tau*/+, blue = *tau/tau*, and gree*n* = wt. Results are plotted as means ± SE at 4 and 17 mo of age (see Tables 1–3 for data). Plasma and/or urinary biochemistry levels remain normal in *tau*/+ maintained on the 22-h LD cycle compared with the abnormal levels for *tau*/+ on 24-h LD (as in Fig. 3*A* and Table 3). **P* < 0.01 evaluated by ANOVA.

animals (Fig. 3*B*). These findings are consistent with the high protein concentrations in the urine, and with the severe renal phenotype. We noted one gel band on SDS-PAGE that consistently appeared in the urine samples analyzed from 17-mo *tau*/+ animals. This band appeared at a molecular mass of ~15 kDa (Fig. 3*B*). To identify the protein in this band, we use mass spectrometry proteomics. The gel band is excised, trypsin digested, and injected by electron spray ionization in an LCQ DECA XP ion trap MS/MS. The identity is confirmed by database searching against hamster, murine, and human databases and by molecular mass comparisons and detection from multiple samples. The ~15-kDa band was identified by MS/MS as cytochrome *c*, which is normally located in the mitochondria of cells. However, release of cytochrome *c* from the inner mitochondrial membrane results in nuclear apoptosis. A representative MS/MS spectrum for cytochrome *c* is shown (Fig. 3*C*).

Because cytochrome *c* release from mitochondria is indicative of cellular apoptosis, this provides a possible mechanism for renal tissue damage in the *tau*/+ animal. Thus we further investigate by assaying the renal tissue for apoptosis, using the TUNEL assay, a common method for detecting DNA fragments resulting from apoptotic signaling cascades. We observe positive staining in *tau*/+ mutant kidney (Fig. 3*D*), indicative of apoptosis and consistent with our findings of urinary cytochrome *c* and with the severe renal phenotype. Clinically, these findings are interesting because cardiovascular disease and kidney disease very often are associated in humans.

We then test the notion that circadian rhythm disruption alone can be responsible for the abnormal cardiorenal phenotype by maintaining *tau*/+ hamsters from 4 mo of age (a time at which heart disease is not yet evident). In one experiment, we raise animals in a phenotype-appropriate 22-h LD cycle (12:10). We retained 10 h of darkness to ensure that a consolidation of nocturnal-type behavior is not an artifact of exposure to very short nights. Behavioral analysis demonstrates that temporal profiles in *tau*/+ are similar in 12:10 LD as in total darkness where the endogenous period of ca. 22 h is expressed (Fig. 4*A*). At 17 mo of age, animals are reexamined, and remarkably the abnormal cardiac and renal phenotypes are both completely absent. This is confirmed by gross morphology, histopathology, plasma biochemistry, urinalysis, and cardiac function using echocardiography and in vivo hemodynamics. Thus all measurements taken from the *tau*/+ group on 22-h days are similar to the wild type and are statistically and "clinically" different from the *tau*/+ group raised on 24-h days (for pathology see Fig. 4, *B-D*; for pathophysiology see Fig. 4, *E-H*; data for 22 h *tau*/+ are listed in Table 1).

In a second experiment, we ablate the SCN, thereby removing the influence of the master circadian oscillator over the peripheral oscillators in heart and kidney. Physiological parameters were not measured in these animals, since the circadian phase of cardiovascular rhythm cannot be determined. However, heart weight-to-body weight ratios are significantly higher in *tau*/+ than wild-type animals held in the 14:10 LD condition, as expected. However, arrhythmic SCN-lesioned *tau*/+ animals have significantly lower ratios than the intact *tau*/+ animals and are not different from the wild type (Fig. 5).

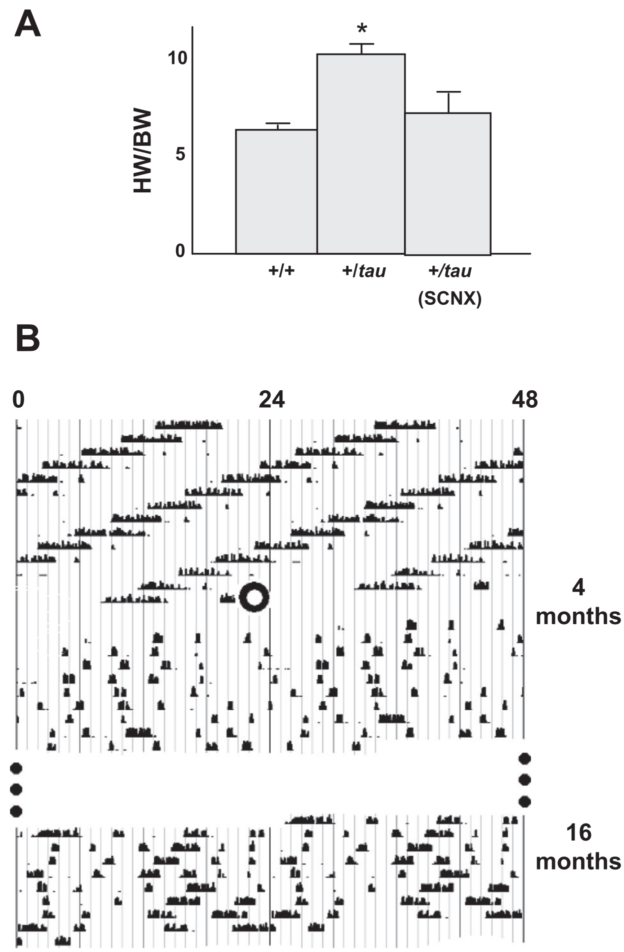

Fig. 5. Suprachiasmatic nucleus (SCN) lesions prevent or reverse circadian rhythm-related cardiac hypertrophy. The SCN in young adult hamsters (6 mo of age) carrying the *tau* mutation (+*/tau)* are electrically ablated, and then animals are maintained in a 14:10 LD cycle thereafter. When animals are close to death as determined by animal care staff, they are removed and killed, and the heart-to-body weight ratio (HW/BW) is determined. Control animals are wt and intact *tau*/+ housed side by side in the same lighting conditions; *n* = 6/group. *A*: HW/BW ratios for wt, +/*tau* (intact), and +/*tau* (SCN ablation). The effectiveness of SCN lesions are verified by the lack of rhythmic wheel running behavior. *B*: actogram showing the immediate (4 mo) and long-term (16 mo) result of the lesion. Animals are housed in 14:10 LD following surgery.

DISCUSSION

The data presented here are consistent with the general hypothesis that diurnal cycling plays a key role in organ growth and renewal and that disruption is a key contributor to disease. Demonstration of abnormal entrainment in *tau*/+ hamsters leading to cardiomyopathy is novel. We postulate that prolonged external endocrine and/or neural cues, through the daily resetting of the clock, play a critical role in triggering the procardiomyopathic response. The discovery of a concomitant renal pathology suggests that circadian disorganization has pervasive effects on organ health. Certainly, the presence of molecular circadian clocks has been demonstrated in several peripheral tissues (5). A recent report that circadian clocks provide temporal organization for the proliferation of renal tubular epithelial cells (12) may give us perhaps some insight into the origins of the urinary cytochrome *c* marker, cortical cell apoptosis, and renal pathology.

It is important to recognize that the key factor in producing cardiovascular disease may not be disruption of the tissue molecular clock per se but the global disturbance or desynchrony that results from the presence of oscillators that are attempting to operate at two distinct periods. That is, in the *tau*/+ heterozygotes, rhythms in peripheral tissues are being produced not only by the intrinsic 22-h molecular oscillator but also by 24 h signals from the SCN, which is being driven by the LD cycle. When the SCN is influenced by a 22-h LD cycle, cardiovascular disease does not develop, as our data show.

The alternative, that the mutated *casein kinase epsilon* gene causes the cardiorenal pathology, seems unlikely. Reversal of disease phenotype following manipulations by circadian principles would not be likely if it was a gene effect, nor would disease pathophysiology be confined to the heterozygote phenotype. The rationale is best illustrated both by the pathological findings and also the physiological parameters represented in Fig. 4. These show that it is only the *tau*/+ animals, and only those aged in the desynchronous 24-h environment, that develop cardiorenal disease. Additional support comes from when *tau*/+ hamsters are influenced by constant light; longevity is similar to the wild type (7). Finally, we further show here that, when the SCN is ablated in *tau*/+ heterozygotes, the influence of the SCN is removed, and presumably the peripheral oscillators become free to operate at their intrinsic period defined by their molecular clock. Thus, collectively, the findings in this study show that, in the absence of the SCN, the peripheral oscillators are free to operate as though they are in constant conditions. In the presence of disruptive signals from the SCN, this disturbs organ structure and function, producing cardiorenal disease and leading to reduced longevity.

The downstream biochemical effects of clock disruption in heart and kidney are not defined. As yet, we have only embryonic knowledge of the steps by which clock time is actually translated into the molecular events that control cell structure and function and, in particular, in the cardiorenal system. One possible candidate link is through perturbation of the glycogen synthase kinase-3β (GSK3β) system; it plays an important regulatory role in cardiac hypertrophy through the stabilization or degradation of β-catenin via ubiquitination and the 26S proteasome (1, 8–10). We speculate on the GSK3β molecule as one potential avenue for future investigation, since it has also most recently been reported to be involved in modulation of the circadian molecular clock pathways; however, further investigation is beyond the scope of this study. Additional and possibly congruent pathways may involve the cardiomyocyte clock and myocardial metabolism, as is being pursued by others (4). Finally, we recently report that circadian rhythm disruption exacerbates preexisting heart disease in a murine model of pressure overload hypertrophy (15), mediated in part by altered rhythmic gene expression. It is also likely that altered autonomic bias, and especially cardiac sympathetic tone, and cycling of neurohormones relevant to the cardiovascular system play a role; these clearly warrant future investigation. Further support of this notion of an autonomic bias or possibly even sympathetic neurotransmitters acting on cardiomyocytes has been suggested by studies using myocyte culture in vitro (3). Moreover, neuro/hormonal factors are also implicated as major contributors to the circadian timing of onset of adverse cardiovascular events such as myocardial infarction and sudden cardiac death. Thus, taken together, our findings support the notion that, not only is physiology rhythmic, but they furthermore illustrate that the processes that trigger compensatory changes in cardiovascular disease are rhythmic as well.

Circadian coordination of daily physiology is critical to the integrity of peripheral organs such as the heart and kidney. The results of these studies suggest that the long-term disruption of circadian rhythms, for example in shift workers, transoceanic flight attendants, or patients with sleep disturbances, can ultimately result in heart and kidney disease. These results have enormous implications for public health and the pathogenesis of cardiac and renal disease; they indicate that maintaining normal circadian rhythms may be an important long-term lifestyle measure for the prevention of these diseases.

Perspectives and Significance

Circadian rhythmicity has been extensively characterized at the level of the SCN, followed by recent investigations that add focus to the peripheral system. It is widely suggested that circadian rhythms of behavior and physiology play a crucial role in integrative physiology, and concomitant organ health and integrity. The cardiovascular system is of particular interest as downstream target of circadian regulation, as has been indicated in numerous epidemiological and clinical physiology reports. We now demonstrate experimentally that normal cardiac physiology, and conversely development of cardiac pathophysiology, may be explained by coincidence between internal and external circadian cues. This is shown in *tau*/+ hamsters, in which there is desynchrony between the 22-h internal endogenous clock system and entrainment to the external 24-h LD environment. Furthermore, these data support the very recent notion demonstrated using algae and plants (13, 17, 22) that circadian regulation is integral to the fitness and growth of an organism. Thus this study shows that circadian dysregulation (desynchrony between the internal circadian clock system and entrainment to normal LD) can play an etiological role in the development of cardiac disease.

ACKNOWLEDGMENTS

We thank Dr. Z. Jia, J. Chalmers, O. Rawashdeh, and K. Varano for technical assistance.

Present address for M. R. Ralph: Centre for Biologic Timing and Cognition, Department of Psychology, SSH 4017, University of Toronto, Ontario, Canada (e-mail: ralph.mr@gmail.com).

GRANTS

This work was supported by the A. Ephriam and Shirley Diamond Cardiomyopathy Research Fund, a grant from the Heart and Stroke Foundation of Ontario (T4479) to M. J. Sole and a grant from the Natural Sciences and Engineering Research Council of Canada to M. R. Ralph.

REFERENCES

1. **Antos CL, McKinsey TA, Frey N, Kutschke W, McAnally J, Shelton JM, Richardson JA, Hill JA, Olson EN.** Activated glycogen synthase-3 beta suppresses cardiac hypertrophy in vivo. *Proc Natl Acad Sci USA* 99: 907–912, 2002.
2. **Bradley TD, Floras JS.** Sleep apnea and heart failure. Part II. Central sleep apnea. *Circulation* 107: 1822–1826, 2003.
3. **Durgan DJ, Hotze MA, Tomlin TM, Egbejimi O, Graveleau C, Abel ED, Shaw CA, Bray MS, Hardin PE, Young ME.** The intrinsic circadian clock within the cardiomyocyte. *Am J Physiol Heart Circ Physiol* 289: H1530–H1541, 2005.
4. **Durgan DJ, Trexler NA, Egbejimi O, McElfresh TA, Suk HY, Petterson LE, Shaw CA, Hardin PE, Bray MS, Chandler MP, Chow CW,**

Young ME. The circadian clock within the cardiomyocyte is essential for responsiveness of the heart to fatty acids. *J Biol Chem* 281: 24254–24269, 2006.

5. **Fukuhara C, Tosini G.** Peripheral circadian oscillators and their rhythmic regulation. *Front Biosci* 8: d642–d651, 2003.
6. **Furlan R, Barbic F, Piazza S, Tinelli M, Seghizzi P, Malliani A.** Modifications of cardiac autonomic profile associated with a shift schedule of work. *Circulation* 102: 1912–1916, 2000.
7. **Guo YF, Stein PK.** Circadian rhythm in the cardiovascular system: chronocardiology. *Am Heart J* 145: 779–786, 2003.
8. **Haq S, Michael A, Andreucci M, Bhattacharya K, Dotto P, Walters B, Woodgett J, Kilter H, Force T.** Stabilization of beta-catenin by a Wnt-independent mechanism regulates cardiomyocyte growth. *Proc Natl Acad Sci USA* 100: 4610–4615, 2003.
9. **Hardt SE, Sadoshima J.** Glycogen synthase kinase-3beta: a novel regulator of cardiac hypertrophy and development. *Circ Res* 90: 1055–1063, 2002.
10. **Hino S, Michiue T, Asashima M, Kikuchi A.** Casein kinase I epsilon enhances the binding of Dvl-1 to Frat-1 and is essential for Wnt-3a-induced accumulation of beta-catenin. *J Biol Chem* 278: 14066–14073, 2003.
11. **Hurd MW, Ralph MR.** The significance of circadian organization for longevity in the golden hamster. *J Biol Rhythms* 13: 430–436, 1998.
12. **Ito T, Ishida N.** Circadian rhythm orchestrates the cell cycle of rat renal epithelial cells: a novel mechanism to regulate the cell cycle (Abstract). *Kidney Int* 68: 1965, 2005.
13. **Johnson CH.** Endogenous timekeepers in photosynthetic organisms. *Annu Rev Physiol* 63: 695–728, 2001.
14. **Martino T, Arab S, Straume M, Belsham DD, Tata N, Cai F, Liu P, Trivieri M, Ralph M, Sole MJ.** Day/night rhythms in gene expression of the normal murine heart. *J Mol Med* 82: 256–264, 2004.
15. **Martino T, Tata N, Belsham DD, Chalmers J, Straume M, Lee P, Pribiag H, Khaper N, Liu PP, Dawood F, Backx PH, Ralph MR, Sole MJ.** Disturbed diurnal rhythm alters gene expression and exacerbates cardiovascular disease with rescue by resynchronization. *Hypertension* 49: 1–10, 2007.
16. **Muller JE, Tofler GH, Stone PH.** Circadian variation and triggers of onset of acute cardiovascular disease. *Circulation* 79: 733–743, 1989.
17. **Nozue K, Covington MF, Duek PD, Lorrain S, Fankhauser C, Harmer SL, Maloof JN.** Rhythmic growth explained by coincidence between internal and external cues. *Nature* 448: 358–361, 2007.
18. **Osiel S, Golombek DA, Ralph MR.** Conservation of locomotor behavior in the golden hamster: effects of light cycle and a circadian period mutation. *Physiol Behav* 65: 123–131, 1998.
19. **Penev PD, Kolker DE, Zee PC, Turek FW.** Chronic circadian desynchronization decreases the survival of animals with cardiomyopathic heart disease. *Am J Physiol Heart Circ Physiol* 275: H2334–H2337, 1998.
20. **Ralph MR, Menaker M.** A mutation of the circadian system in golden hamsters. *Science* 241: 1225–1227, 1988.
21. **Storch KF, Lipan O, Leykin I, Viswanathan N, Davis FC, Wong WH, Weitz CJ.** Extensive and divergent circadian gene expression in liver and heart. *Nature* 417: 78–83, 2002.
22. **Woelfle MA, Ouyang Y, Phanvijhitsiri K, Johnson CH.** The adaptive value of circadian clocks: an experimental assessment in cyanobacteria. *Curr Biol* 14: 1481–1486, 2004.
23. **Young ME, Razeghi P, Cedars AM, Guthrie PH, Taegtmeyer H.** Intrinsic diurnal variations in cardiac metabolism and contractile function. *Circ Res* 89: 1199–1208, 2001.
24. **Young ME, Razeghi P, Taegtmeyer H.** Clock genes in the heart: characterization and attenuation with hypertrophy. *Circ Res* 88: 1142–1150, 2001.